Journal of Applied Electrochemistry (2006) 36:1163–1168
DOI 10.1007/s10800-006-9204-1

Eco friendly corrosion inhibitors: Inhibitive action of quinine for corrosion of low carbon steel in 1 M HCl

MOHAMED ISMAIL AWAD
Chemistry Department, Faculty of Science, Cairo University, Cairo, Egypt
*(*author for correspondence, tel.: + 202-5676603; fax: + 202-5685799; e-mail: mawad70@yahoo.com)*

Received 5 January 2006; accepted in revised form 3 July 2006

Key words: adsorption, corrosion inhibitors, electrochemical impedance spectroscopy, quinine, steel

Abstract

Quinine, a natural product, was investigated as a corrosion inhibitor for low carbon steel in 1.0 M HCl solution. Electrochemical impedance spectroscopy (EIS) and potentiodynamic polarization were used to study the inhibition action in the temperature range 20–50 °C. The corrosion of steel was controlled by a charge transfer process at the prevailing conditions. The electrochemical results showed that quinine is an efficient inhibitor for low carbon steel and an efficiency up to 96% was obtained at 20 °C. The inhibition efficiency increases with inhibitor concentration and reaches a near constant value in the concentration range 0.48 mM and above. Application of the Langmuir adsorption isotherm enabled a study of the extent and the mode of adsorption.

1. Introduction

Organic inhibitors have long been used for industrial acid cleaning, oil well acidification and acid pickling and descaling [1, 2]. For these applications HCl is considered to be superior and more economical than H_2SO_4 [3]. A number of compounds containing nitrogen and/or sulphur have been studied as corrosion inhibitors and have shown excellent performance [4–14]. However, the environmental impact of these inhibitors has been considered in the recent decades due to their toxic effects on aquatic and possibly animal life [15].

Currently, research is focusing on producing and testing environmentally friendly corrosion inhibitors [16]. Few studies report the use of natural products as corrosion inhibitors [17–20]. In the present work, the feasibility of using quinine sulfate, a natural product, as a non-toxic inhibitor for the inhibition of the corrosion of low carbon steel in 1M HCl is examined. Potentiodynamic polarization and electrochemical impedance spectroscopy (EIS) are used for this purpose. The extent and mode of adsorption of quinine on steel are discussed on the basis of applying adsorption isotherms.

2. Experimental

Analytical grade chemicals and triple distilled water were used for the preparation of all solutions. The electrolyte solution was 1.0 M HCl. Quinine sulphate of structure shown in Figure 1 was used as inhibitor.

The low carbon steel sample was of composition (wt. %): 0.1 C, 0.29 Mn, 0.07 Si, 0.012 S, 0.021 P, the balance being Fe. The working electrode was in the form of a rod machined into a cylindrical form embedded in epoxy resin leaving an open surface area of 1 cm^2. Prior to measurements it was pretreated by mechanical polishing with emery papers of different grades up to 4/0 grit, degreased with ethanol, washed with tridistilled water and then dried at room temperature before use. Electrochemical measurements were conducted in a conventional three-electrode thermostated cell assembly using an EG&G potentiostat (model 273A) and a lock-in amplifier (model 5210), operated with Corr 352 and EIS M398 software. A platinum spiral wire and standard calomel electrode (SCE) were used as counter and reference electrodes, respectively. The potentiodynamic current–potential curves were obtained at a scan rate of 1 mV s^{-1}. EIS measurements were carried out in the frequency range 100 kHz to 10 mHz with amplitude of 5 mV peak-to-peak using a.c. signals at open circuit potential. In all experiments electrochemical measurements were started about 30 min after the working electrode was immersed in solution to allow a stabilization of the steady state potential. All potentials were measured against SCE.

3. Results and discussion

3.1. *Electrochemical impedance spectroscopy*

The corrosion behavior of low carbon steel in 1 M HCl in the presence and absence of quinine of various

concentrations were investigated by EIS. All impedance spectra were measured at the respective corrosion potential.

The Nyquist representation of low carbon steel in 1 M HCl both in the absence and presence of quinine of various concentrations is shown in Figure 2. The impedance parameters derived from this figure are given in Table 1. A single semicircle loop is observed for the blank response which is unaffected by the inhibitor concentration indicating the activation controlled nature of the reaction with one charge transfer process [21, 22]. The semicircle diameter is significantly increased with increasing quinine concentration indicating its high inhibition efficiency. The semicircle is of slightly depressed nature and has a center below the x-axis. Such a depression is characteristic of solid electrodes and is often ascribed to dispersing effects, which have been attributed to roughness and inhomogenities of the surface during corrosion [21, 22]. Increase in inhibitor concentration does not affect the profile of the impedance behavior suggesting the same mechanism as in the absence of inhibitor. The charge transfer resistance values were calculated from the difference in impedance at lower and higher frequencies [23, 24]. The charge transfer resistance (R_t) is considered to be equivalent to the polarization resistance which is inversely proportional to corrosion rate. The double layer capacitance was estimated from the following equation:

$$C_{dl} = \frac{1}{2\pi f_{max} R_t} \quad (1)$$

where f_{max} is the frequency corresponding to the maximum imaginary component of the impedance. The inhibition efficiency was calculated using the charge transfer resistance [25]:

$$\text{Inhibition efficiency} = (1 - \frac{R_t}{R_t'})100 \quad (2)$$

where R_t and R_t' are the charge transfer resistance values without and with the inhibitor, respectively. Inspection of Figure 1 and Table 1 indicates that the values of C_{dl} are reduced in the presence of inhibitor. Increasing the quinine concentration leads to a decrease in C_{dl} and an increase in inhibition efficiency. This decrease in C_{dl} may result from a decrease in local dielectric constant and/or an increase in the thickness of the electrical double layer

Table 1. Effect of concentration of quinine on characteristic parameters evaluated from EIS for steel in 1 M HCl and the corresponding corrosion inhibition efficiency

C/mM	Charge transfer resistance R_{ct}/ Ψ cm^2	Double layer capacitance, C_{dl}/μF cm^{-2}	Inhibition efficiency/%
0	182	32.3	
0.08	568	25.5	68
0.15	1048	22.6	83
0.24	1437	21.2	87
0.48	2336	16.6	92
0.8	3488	9.7	95

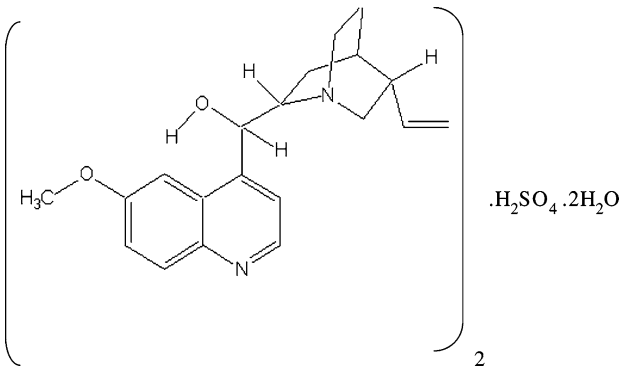

Fig. 1. Molecular structure of quinine sulphate.

suggesting that the inhibitor exerts its action via adsorption at the solution/interface [26–28].

3.2. *Potentiodynamic polarization*

Figure 3 shows polarization curves for low-carbon steel in 1 M HCl in the presence of different quinine concen-

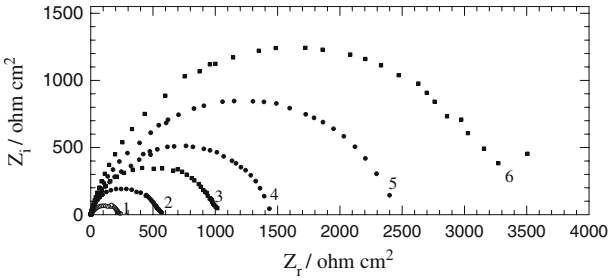

Fig. 2. Nyquist diagrams of steel electrode in 1.0 M HCl containing various concentrations of quinine: (1) 0.0, (2) 2×10^{-5}, (3) 8×10^{-5}, (4) 2.4×10^{-4}, (5) 4.8×10^{-4} and (6) 8.0×10^{-4} M.

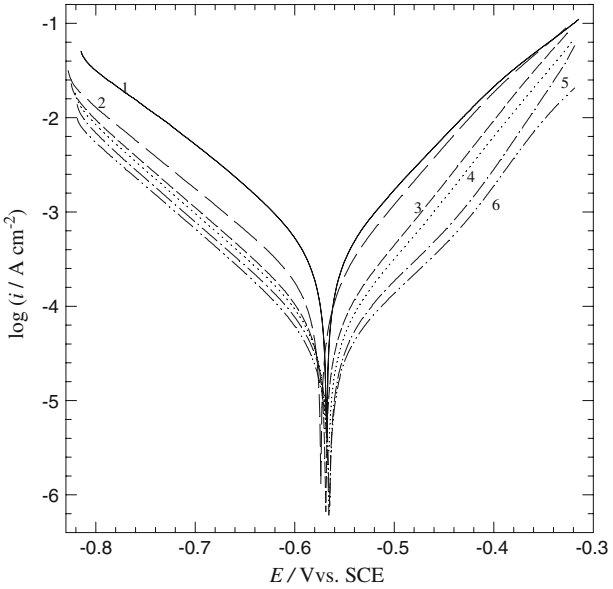

Fig. 3. Polarization curves for low carbon steel in 1 M HCl containing various concentrations of quinine: (1) 0.0, (2) 2×10^{-5}, (3) 8×10^{-5}, (4) 2.4×10^{-4}, (5) 4.8×10^{-4} and (6) 8.0×10^{-4} M at 20 °C.

Table 2. Corrosion potential E_{corr}, anodic and cathodic Tafel slopes b_a and b_c, corrosion current densities (i_{corr}) and the degree of surface coverage (θ in the presence and absence of different concentrations of quinine at different temperatures

T °C	C / mM	E_{corr} / Mv	b_a / mV dec^{-1}	b_c / mV dec^{-1}	i_{corr} / μA cm^{-2}	θ
20	0	576	125	126	366	
	0.08	563	112	90	139	0.62
	0.11	560	107	79	86	0.84
	0.24	568	99	73	44	0.88
	0.48	568	99	73	26	0.93
	0.8	568	99	71	15	0.96
30	0	568	125	106	600	
	0.08	574	114	95	270	0.55
	0.11	569	106	77	162	0.73
	0.24	567	106	77	126	0.79
	0.48	565	106	68	90	0.85
	0.8	559	114	63	66	0.89
40	0	572	136	96	1649	
	0.08	575	127	91	844	0.49
	0.11	581	123	77	574	0.65
	0.24	579	125	83	474	0.71
	0.48	588	124	110	346	0.79
	0.8	589	125	147	330	0.82
50	0	564	143	98	1990	
	0.08	574	138	87	1134	0.43
	0.11	576	135	72	809	0.59
	0.24	576	134	72	656	0.67
	0.48	571	133	78	535	0.72
	0.8	574	147	97	530	0.75

trations at 20 °C. The cathodic and anodic polarization curves are shifted to lower currents in the presence of quinine. The shift is dependent of concentration. At lower concentration, the shift in the cathodic Tafel line is more pronounced than that in the anodic branch. In general the inhibitor acts as a mixed type inhibitor. Polarization curves at 30, 40 and 50 °C were also obtained and analyzed to extract the electrochemical parameters. These are shown in Table 2. The values of corrosion current densities were obtained by Tafel extrapolation method. From the values of the cathodic Tafel slope (b_c) and anodic Tafel slope (b_a), it may be concluded that the addition of quinine does not change the mechanism of both hydrogen evolution and iron dissolution. That is to say, the inhibition action of quinine is by simple blocking of the metal surface. The corrosion potential (E_{corr}) is almost constant which is in agreement with the above conclusion that the inhibitor is a mixed type inhibitor.

The inhibition efficiency for the corrosion reaction (P_{icorr}) was calculated from the following equation [29]:

$$P_{icorr} = \left(\frac{i_1 - i_2}{i_1}\right) 100 \quad (3)$$

where i_1 and i_2 are the corrosion current densities in the absence (blank) and in the presence of quinine, respectively. Figure 4 shows the inhibition efficiency at different inhibitor concentrations and at different temperatures. P_{icorr} increases with inhibitor concentration and semi-constant values are obtained at different temperatures when the inhibitor concentration attains a value of about 0.48 mM. At constant inhibitor concentration, upon increasing the temperature, the inhibition efficiency decreases. The decrease in inhibition efficiency with increasing temperature may be due to the increase in quinine desorption [30]. Adsorption isotherms could quantify this effect. The polarization measurements are in agreement with the impedance results obtained at 20 °C as can be seen from the agreement between the inhibition efficiencies determined by both techniques (Tables 1 and 2).

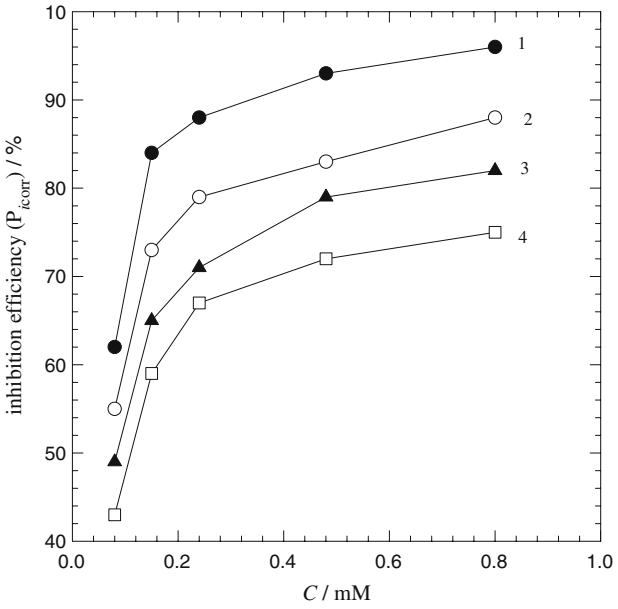

Fig. 4. Inhibition efficiency at different concentrations of quinine for low carbon steel in 1 M HCl at different temperatures: (1) 20, (2) 30, (2) 40 and (4) 50 °C.

3.3. *Adsorption isotherms*

The mode and extent of the interaction between inhibitor and the iron surface can be studied by applying adsorption isotherms. The degree of surface coverage, θ, at different inhibitor concentrations in 1 M HCl was evaluated from polarization measurements (θ = P_{icorr}/100) and is given in Table 2. The fitting to the Langmuir isotherm is shown by plotting C/θ versus C (Figure 5) according to the following equation [31, 32]:

$$\frac{C}{\theta} = \frac{1}{K} + C \quad (4)$$

where K is the adsorption equilibrium constant. In this case, linear plots with high correlation coefficients and slopes of 1.0 ± 0.1 were obtained at different temperatures indicating that the experimental results fit the Langmuir isotherm. The values of the correlation coefficients and the adsorption equilibrium constants are given in Table 3. Free energy of adsorption can be determined with Equation (5).

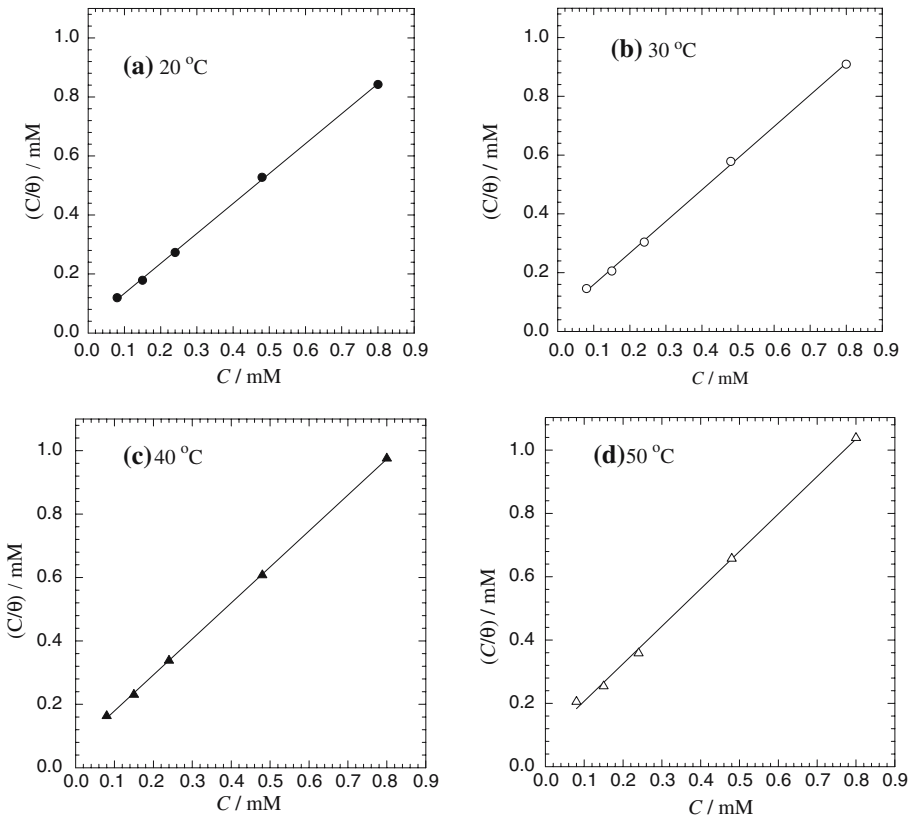

Fig. 5. Langmuir adsorption isotherm plots for the adsorption of quinine in 1 M HCl at temperatures (a) 20, (b) 30, (c) 40 and (d) 50 °C.

$$K = \frac{1}{55.5}\exp\left(\frac{-\Delta G^{o}_{ads}}{RT}\right) \quad (5)$$

where ΔG^{o}_{ads} is the standard free energy of adsorption and the value of 55.5 is the concentration of water in solution expressed in mol. The decrease in K with increasing temperature indicates a decrease in the extent of adsorption with increasing temperature [33]. There are many possibilities regarding the mode of adsorption of quinine on steel. The most probable one is adsorption through bridged chloride [16, 34, 35] since under the present experimental conditions quinine is in the cationic form and the iron surface is considered to be positively charged [36, 37]. It is noteworthy that the inhibitive action of quinine on the corrosion of low carbon steel in H_2SO_4 is almost nil (data are not shown here). This indicates that the adsorption of quinine via a chloride bridge is the most probable mode of adsorption.

3.4. *Thermodynamic parameters for quinine adsorption*

Thermodynamic parameters including heat of adsorption, adsorption free energy and the adsorption entropy are important in the elucidation of the inhibition mechanism. The heat of adsorption (ΔH^{o}_{ads}) can be obtained using the Van't Hoff equation [31]:

$$\ln K = \left(\frac{-\Delta H^{o}_{ads}}{RT}\right) + \text{constant} \quad (6)$$

By plotting *ln K* vs. $1/T$, ΔH_{ads} can be obtained from the slope and then the entropy of adsorption can be obtained at various temperatures using the equation $\Delta G^{o}_{ads} - \Delta H^{o}_{ads} - T\Delta S^{o}_{ads}$. Figure 6 shows the relation between *ln K* and $1/T$ and the thermodynamic parameters obtained are given in Table 4. The negative values for ΔG^{o}_{ads} ensure the spontaneity of the adsorption of quinine on steel and that adsorption is stable in the studied temperature range. It is reported that values of

Table 3. Some parameters of the linear regression between θ and log *C*

Temperature K	Ln/*K* L mol^{-1}	Correlation coefficient
293	3.42	0.99
303	2.96	0.99
313	2.72	0.99
323	2.43	0.99

Table 4. The thermodynamic parameters of adsorption of quinine on the steel surface at different temperatures

Temperature/K	ΔG^{o}_{ads} k/ J mol^{-1}	ΔH^{o}_{ads}/ kJ mol^{-1}	ΔS^{o}_{ads}/ J mol^{-1} K^{-1}
293	− 18.08	− 25.3	− 25
303	− 17.54	− 25.3	− 26
313	− 17.49	− 25.3	− 25
323	− 17.28	− 25.3	− 25

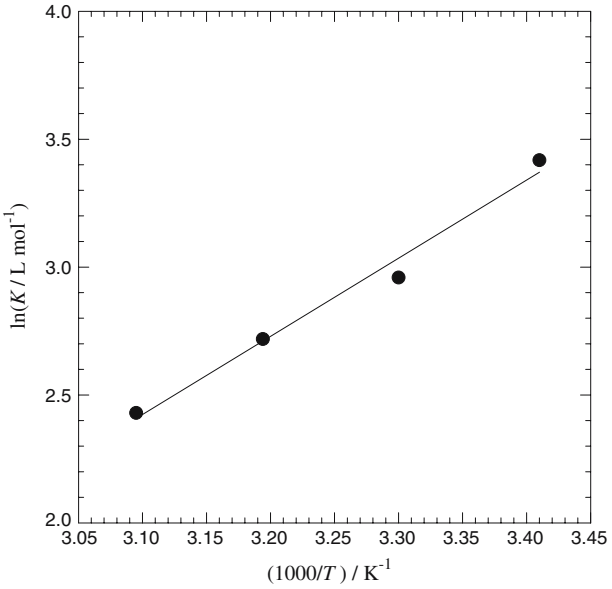

Fig. 6. The relationship between *ln K* and $1/T$.

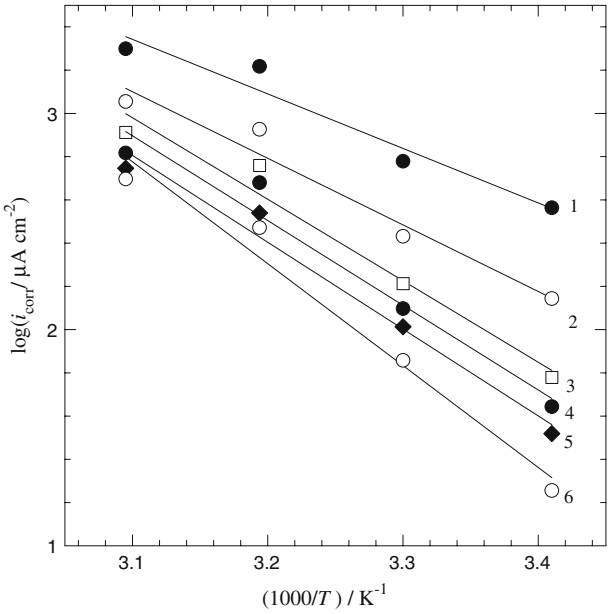

Fig. 7. Arrhenius plots of low-carbon steel in 1 M HCl in the absence and presence of different concentrations (M) of quinine: (1) 0.0, (2) 2×10^{-5}, (3) 8×10^{-5}, (4) 2.4×10^{-4}, (5) 4.8×10^{-4} and (6) 8.0×10^{-4} M.

ΔG^{o}_{ads} up to -20 kJ mol^{-1} are characteristic for physisorption, i.e., electrostatic interaction between the charged molecules and the charged surface [38, 39]. A value of -17 ± 1 kJ mol^{-1} may indicate a physisorption. The decrease in inhibition efficiency with increasing temperature confirms the physisorption mode (as discussed in Figure 4). ΔH^{o}_{ads} is another criterion from which the mode of adsorption can be probed. Generally, an endothermic process is explicit to chemisorption while an exothermic adsorption process designates either physi- or chemisorption [40]. In exothermic adsorption, the adsorption mode is judged based on the absolute value of ΔH^{o}_{ads}. Enthalpy of adsorption of absolute values lower than 41.86 kJ mol^{-1}indicate physisorption and values approaching 100 kJ mol^{-1} indicate chemisorption [41]. In the present case, the absolute values of enthalpy are lower than 41.86 kJ mol^{-1}confirming physisorption. The negative values of ΔS^{o}_{ads} (shown in Table 4) are expected as the adsorption process is accompanied by a decrease in the disorder of the system due to the adsorption of the free bulky quinine molecules onto the electrode surface.

3.5. *Kinetic parameters*

The quantification of the effect of temperature on the corrosion current density can be expressed by the Arrhenius equation [42]:

$$i_{corr} = A \exp\left(\frac{-E_a}{RT}\right) \quad (7)$$

where i_{corr} is the reaction rate, A is the Arrhenius pre-exponential constant, E_a the activation energy of the corrosion reaction, T the absolute temperature and R the universal gas constant. Figure 7 depicts an Arrhenius plot (corrosion rate against the reciprocal of temperature ($1/T$)) for low-carbon steel in 1 M HCl solution in the absence and presence of different quinine concentrations. Satisfactory straight lines of high correlation coefficients are obtained and the activation energy can be obtained from the slopes. The activation energies obtained are given in Table 5. The apparent activation energy obtained for corrosion process was found to be 45.2 kJ mol^{-1}. It is clear that E_a values in the presence of inhibitors are much higher than those in the absence of inhibitor. The higher activation energies mean a slow reaction and that the reaction rate is very sensitive to temperature. The increase in apparent activation energy in the presence of quinine denotes physical adsorption [43]. This conclusion is denoted by the decrease in the inhibition efficiency with increasing temperature (Figure 4) and from the values of ΔH^{o}_{ads}. Moreover, the increase in activation energy is proportional to the inhibitor concentration, indicating that the energy barrier for the corrosion process is also increased [4]. The increase in activation energy with inhibitor concentration is often interpreted by physical adsorption with the formation of an adsorptive film of an electrostatic character [43].

Table 5. Activation parameters for the dissolution reaction of steel in 1.0 M HCl in the presence and absence of quinine of different concentrations

C (mM)	E_a/kJ mol^{-1}
0.0	45.2
0.08	58
0.11	71.6
0.24	74.7
0.48	82.5
0.8	97.5

4. Conclusions

The results of this study lead to the following conclusions:

1. Quinine acts as an efficient inhibitor for the corrosion of steel in 1 M HCl in the studied temperature range. It exerts its action via simple adsorption following the Langmuir adsorption isotherm.
2. The adsorption is of physisorption type as indicated from different adsorption parameters, i.e., ΔG°_{ads}, ΔH°_{ads} and ΔS°_{ads}.
3. EIS measurements indicate that the corrosion of iron is controlled by a one charge transfer process.

References

1. G. Schmitt, *Brit. Corros. J.* **19** (1984) 165.
2. G. Lewis, *Br. Corros. J.* **16** (1981) 169.
3. S. Sathiyanarayanan, C. Marikkannu and N. Palaniswamy, *App. Surf. Sci.* **241** (2005) 477.
4. F. Zucchi, G. Trabanelli and G. Brunoro, *Corros. Sci.* **36** (1994) 1683.
5. B. Mernari, H. Elattari, M. Traisnel, F. Bentiss and M. Lagrenee, Corros. *Sci.* **40** (1998) 391.
6. M. Elachouri, M.S. Hajji, S. Kertit, E.M. Essasi, M. Salem and R. Coudert, *Corros. Sci.* **37** (1995) 381.
7. E. McCafferty, V. Pravdic and A.C. Zettlemoyer, *Trans. Faraday Soc.* **66** (1999) 237.
8. R.C. Ayers Jr. and N. Hackerman, *J. Electrochem. Soc.* **110** (1963) 507.
9. I. Ammar and F.M. El-Khorafi, *Werkst. Korros.* **24** (1973) 702.
10. B.G. Ateya, B.E. El-Anadouli and F.M.A. El-Nizamy, *Bull. Chem. Soc. Jpn.* **54** (1981) 3157.
11. K.C. Pillai and R. Narayan, *Corros. Sci.* **23** (1983) 151.
12. R.M. Oza, P.C. Vadher, A.B. Patel and J.C. Vora, *J. Electrochem. Soc. India* **34** (1985) 143.
13. K.C. Emregül, A.A. Akay and O. Atakol, *Mat. Chem. Phys.* **93** (2005) 325.
14. I. Lukovits, I. Bako, A. Shaban and E. Kalman, *Electrochim. Acta* **43** (1998) 131.
15. D.L. Lake, Corrosion Prevention and Control, 1988, p. 113.
16. K.F. Khaled, *Electrochim. Acta* **48** (2003) 2493.
17. S.-J. You, Y.-S. Choi, J.-G. Kim, H.-J. Oh and C.-S. Chi, *Mat. Sci. Eng. A* **345** (2003) 207.
18. G.N. Mehta and T.P. Sastry, *J. Electrochem. Soc. India* **30** (1981) 284.
19. B. Hammouti, S. Kertit and M. Melhaoui, *Bull. Electrochem.* **11** (1995) 553.
20. B. Hammouti, S. Kertit and M. Melhaoui, *Bull. Electrochem.* **13** (1997) 97.
21. T. Szauer and A. Brandt, *Electrochim. Acta* **26** (1981) 943.
22. T. Paskossy, *J. Electroanal. Chem.* **364** (1994) 111.
23. K. Jutner, *Electrochim. Acta* **35** (1990) 1150.
24. T. Tsuru, S. Haruyama and B. Gijutsu, *J. Jpn. Soc. Corros. Eng.* **27** (1978) 573.
25. L. Elkadi, B. Mernari, M. Traisnel, F. Bentiss and M. Lagrenee, *Corros. Sci.* **42** (2000) 703.
26. E.M.-C. Cafferty and N. Hackerman, *J. Electrochem. Soc.* **119** (1972) 146.
27. F. Bentiss, M. Lagrenee, M. Traisnel and J.C. Hornez, *Corros. Sci.* **41** (1999) 789.
28. I.L. Rosenfeld, *Corrosion Inhibitors* (McGraw-Hill, New York, 1981).
29. J.O'M. Bockris and B. Yang, *J. Electrochem. Soc.* **138** (1991) 2237.
30. E.E. Ebenso, *Nig. Corros. J.* **1** (1998) 29.
31. T.P. Zhao and G.N. Mu, *Corros. Sci.* **41** (1999) 1937.
32. C. Chakrabarty, M.M. Singh, P.N.S. Yadav and C.V. Agarwal, *Trans SAEST* **18** (1983) 15.
33. L. Tang, G. Mu and G. Liu, *Corros. Sci.* **45** (2003) 2251.
34. N. Hackerman and E. McCafferty, *in* Proceedings of the 5th International Congress on Metallic Corrosion, Tokyo, 1972.
35. T. Murakawa, S. Nagaura and N. Hackerman, *Corros. Sci.* **7** (1967) 79.
36. G.N. Mu, T.P. Zhao, M. Liu and T. Gu, *Corrosion* **52** (1996) 853.
37. H. Luo, Y.C. Guan and K.N. Han, *Corrosion* **54** (1998) 721.
38. F. Bentiss, M. Traisnel and M. Lagrenee, *Corros. Sci.* **42** (2000) 127.
39. F. Donahue and K. Nobe, *J. Electrochem. Soc.* **112** (1965) 886.
40. W. Durnie, R.D. Marco, A. Jefferson and B. Kinsella, *J. Electrochem. Soc.* **146** (1999) 1751.
41. S. Martinez and I. Stern, *App. Surf. Sci.* **199** (2002) 83.
42. G. Moretti, G. Quartarone, A. Tassan and A. Zingales, *Electrochim. Acta* **41** (1996) 1971.
43. A. Popova, E. Sokolova, S. Raicheva and M. Christov, *Corros. Sci.* **45** (2003) 33.